ChemComm

COMMUNICATION

View Article Online
View Journal | View Issue



Cite this: *Chem. Commun.*, 2014, **50**, 1341

Received 11th November 2013,
Accepted 26th November 2013

DOI: 10.1039/c3cc48587k

www.rsc.org/chemcomm

# Simultaneous imaging of protonated and deprotonated carbonylcyanide *p*-trifluoromethoxyphenylhydrazone in live cells by Raman microscopy†

Hiroyuki Yamakoshi,[ab] Almar F. Palonpon,[ac] Kosuke Dodo,[ab] Jun Ando,[ac] Satoshi Kawata,[c] Katsumasa Fujita[ac] and Mikiko Sodeoka*[ab]

**We report the simultaneous imaging of protonated and deprotonated forms of carbonylcyanide *p*-trifluoromethoxy-phenylhydrazone (FCCP) molecules in live cells by Raman microscopy. Nitriles, structure-sensitive Raman tags, are used to detect the two distinct molecular structures, demonstrating the potential of Raman microscopy for structure-based imaging of bioactive small molecules.**

Small molecules serve as modulators of a myriad of biological systems by interacting with biomolecules to regulate their functional activities or as sensors of a cellular environment. Consequently, the utilization of biologically active small molecules has resulted in many important advances in our understanding of various cellular processes and has also contributed significantly to drug discovery and development.[1] A method that can image the molecular structures of bioactive small molecules within live cells should provide new insights into many biological functions and processes. Infrared (IR) spectroscopy is one candidate for this purpose,[2] but it is difficult to apply IR methods for live-cell imaging due to interference from the strong absorption band of water and low spatial resolution. Another candidate for structure-based imaging of small molecules is Raman spectroscopy. This technique has been widely used for analysis of molecular structures,[3] and more recently, early work on the detection of structural information of specific molecules in live cells has produced promising results.[4] Recent developments in Raman instrumentation based on parallel detection have made it possible to acquire chemical images of a sample with high spatial and temporal resolution.[5] As a result, Raman microscopy has emerged as a powerful tool for live cell imaging applications. However, overlapping of critical Raman signals from the small molecule of interest with Raman signals from numerous biomolecules in the cell often makes analysis complicated. To overcome this problem, we recently proposed a method for small molecule imaging in live cells by using an alkyne tag (alkyne-tag Raman imaging, ATRI).[6,7]

The concept behind ATRI is to tag molecules with an alkyne moiety whose vibrational frequency lies in the spectroscopically silent region of the cell (between 1800 and 2700 $cm^{-1}$), so that the signal is free from interference with Raman signals of endogenous molecules. The alkyne tag is small enough to minimally perturb the properties of the small molecule. Besides alkyne, nitrile is another small functional groups that show strong Raman signals in the cellular silent region. We studied the relationship between Raman shift/intensity and structure of various alkynes and nitriles and found a strong dependence of the Raman shift frequency of alkyne and nitrile signals on the surrounding chemical structure.[7] This finding suggests that both alkynes and nitriles could be good Raman probes for structure-based imaging of small molecules. Here, we examine the feasibility of employing Raman microscopy to image different structural forms of the same small molecule simultaneously by using the widely used uncoupler, FCCP (carbonylcyanide *p*-trifluoromethoxyphenylhydrazone),[8] as a model system in which the nitrile group serves as an intrinsic Raman tag.

FCCP was first reported in 1962 by Heytler and Prichard.[9] With a slightly acidic proton ($pK_a$ 6.0), FCCP should exist in cells as an equilibrium mixture of deprotonated and protonated forms (Fig. 1). It is believed that both states of FCCP can cross the membrane lipid bilayer, due to the appropriate hydrophobicity ($\log P$ 2.42) and the delocalized anionic character of the molecule, allowing it to act as an uncoupler.[8] Uncouplers are an interesting group of compounds that dissipate the proton gradient across the mitochondrial inner membrane and "uncouple" the function of the electron transport chain from ATP synthesis. Therefore, FCCP has been used for studying mitochondrial functions. Some uncouplers have been used as fungicides, and mild uncouplers are also expected to have therapeutic potential based on the hypothesis that mild uncoupling can be beneficial to cells in certain pathological states.[10] To our

[a] *Sodeoka Live Cell Chemistry Project, ERATO, Japan Sciences and Technology Agency, 2-1 Hirosawa, Wako-shi, Saitama 351-0198, Japan. E-mail: sodeoka@riken.jp*
[b] *Synthetic Organic Chemistry Laboratory, RIKEN, 2-1 Hirosawa, Wako, Saitama 351-0198, Japan*
[c] *Department of Applied Physics, Osaka University, 2-1 Yamadaoka, Suita, Osaka 569-0871, Japan*

† Electronic supplementary information (ESI) available: Experimental procedures and spectral data. See DOI: 10.1039/c3cc48587k

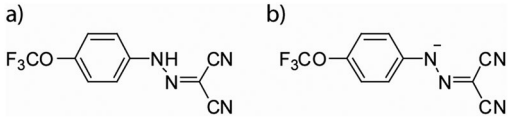


Fig. 1 (a) Protonated and (b) deprotonated forms of FCCP.

knowledge, FCCP has never been previously visualized in live cells. It is anticipated that protonation-state-specific imaging of FCCP could provide invaluable information for medicinal and biological research.

First, the Raman spectra of deprotonated and protonated FCCP in solution were compared to determine the difference of nitrile peak frequencies. The spectra were obtained in aqueous DMSO adjusted to various pH values. Since FCCP has an acidic p$K_a$ of 6.0,[8] it is almost completely protonated at pH 4.6 and almost completely deprotonated at physiological pH (pH 7.4).[11] As shown in Fig. 2, the Raman spectra of deprotonated FCCP showed nitrile Raman signals at 2176 and 2195 cm$^{-1}$ (Fig. 2, red). In contrast, protonated FCCP showed a single strong nitrile signal at 2226 cm$^{-1}$ (Fig. 2, green). Much to our delight, the nitrile bands of the protonated and deprotonated forms were well separated and readily distinguishable in the Raman spectra. In pH 6.0 buffer, all three peaks were observed, indicating that FCCP molecules exist as a mixture of protonated and deprotonated forms at this pH, as expected (ESI,† Fig. S1). In contrast, only the peak of the protonated form was observed in aprotic DMSO without buffer (ESI,† Fig. S2). In addition to the difference of nitrile signals, the two forms showed different signals in the fingerprint region. The Raman spectra of deprotonated FCCP showed distinct Raman bands at 1154, 1319, 1360, and 1494 cm$^{-1}$. These peaks are very weak for protonated FCCP; instead, a characteristic signal at 1511 cm$^{-1}$ was observed (Fig. 2 and ESI,† Fig. S3). Furthermore, two rather similar Raman signals appearing at the same Raman shift frequency, 1298 cm$^{-1}$, were observed in both spectra (Fig. 2). Since these signals could overlap with strong cellular signals that usually appear in this region, the distinct nitrile signals in the cellular silent region were considered more suitable for separately imaging the deprotonated and protonated forms of FCCP molecules in live cells.

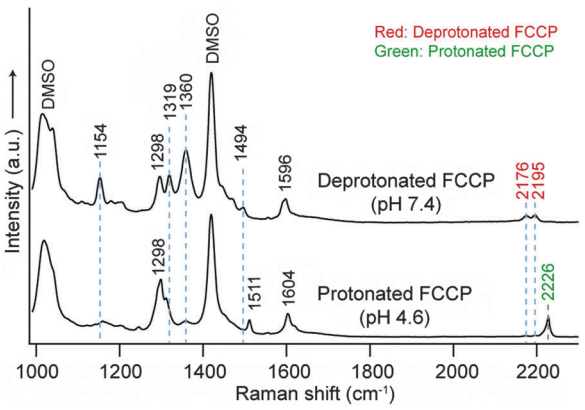


Fig. 2 Raman spectra of protonated and deprotonated FCCP. The sample concentration was 10 mM in DMSO with buffer. The laser wavelength was 532 nm. The light intensity at the sample plane was 3 mW μm$^{-2}$. The exposure time for each line was 10 s.

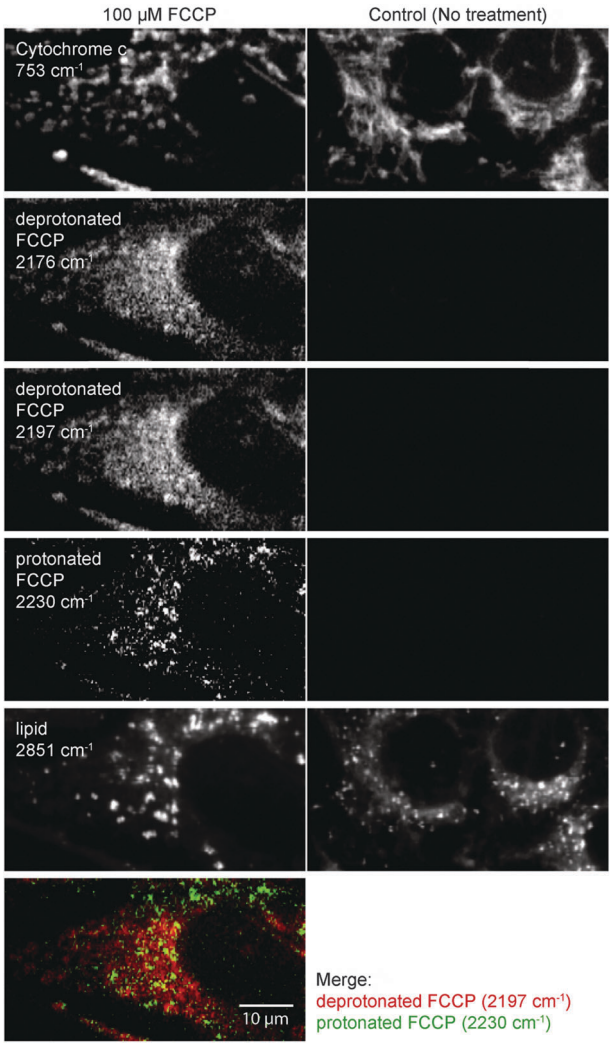


Fig. 3 Raman imaging of protonated and deprotonated forms of FCCP in live HeLa cells. Raman images were obtained from HeLa cells treated with 100 μM FCCP. The signals at 2197 and 2230 cm$^{-1}$ were assigned to the red and green channels, respectively, and a merged image was generated. The laser wavelength was 532 nm. The light intensity at the sample plane was 4.2 mW μm$^{-2}$. The exposure time for each line was 10 s. The total number of lines was 140.

Next, we performed Raman imaging of deprotonated and protonated FCCP molecules in live cells. HeLa cells were incubated with 100 μM FCCP for 30 min, and Raman images were obtained by laser excitation at 532 nm (Fig. 3). Images were constructed from the distribution of Raman peaks at 753, 2176, 2197, 2230 and 2851 cm$^{-1}$. The peaks at 753 and 2851 cm$^{-1}$ are assigned to cytochrome *c* and lipid molecules, respectively.[12] The peaks at 2176 and 2197 cm$^{-1}$ correspond to deprotonated FCCP, while the peak at 2230 cm$^{-1}$ corresponds to protonated FCCP. At a concentration of 100 μM FCCP, the distribution of cytochrome *c* shows granulated structures similar to the reported shapes of mitochondria treated with the uncoupler.[13] Ionic deprotonated FCCP exhibited a diffuse distribution in the cytoplasm, whereas protonated FCCP colocalized with lipid droplets. In lipids, FCCP is held in a hydrophobic environment and hence should

 

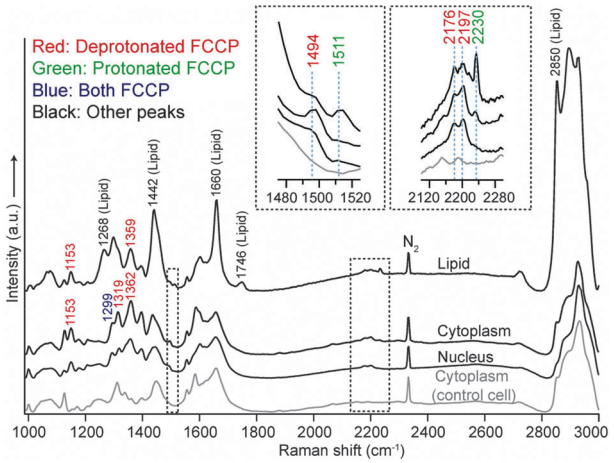


Fig. 4 Average Raman spectra obtained from HeLa cells. Spectra were obtained from a lipid-rich region (10 points) and a cytoplasmic region (10 × 10 pixels) of HeLa cells. The spectra are vertically offset for easy viewing.

favor the protonated form,[10] in accordance with the above results. In the nucleus, deprotonated FCCP can still be observed, albeit with weak contrast.

To further confirm the distributions observed in the Raman images, we examined the average Raman spectra obtained from each cellular component (Fig. 4 and ESI,† Fig. S4). As expected, the cytoplasm showed mostly deprotonated FCCP signals consisting of the nitrile peaks at 2176 and 2197 $cm^{-1}$. In contrast, both deprotonated and protonated (2230 $cm^{-1}$) FCCP signals were observed in lipids. The spectra also confirmed that deprotonated FCCP molecules exist in the nucleus, but almost no protonated FCCP molecules were detected there. Besides the nitrile peaks, the Raman spectra showed several FCCP peaks in the fingerprint region that could also be used to differentiate the protonation state of FCCP, for example, 1494 $cm^{-1}$ for deprotonated FCCP and 1511 $cm^{-1}$ for protonated FCCP. Although the Raman spectra of the mitochondrial membrane could not be detected in this experiment, the detection of both deprotonated and protonated FCCP signals in lipids supports the view that both forms of FCCP can cross hydrophobic lipid membranes in live cells.

In conclusion, we present the first structure-based imaging of different forms of a bioactive small molecule in live cells by using Raman microscopy, which allowed us to simultaneously visualize the distributions of two distinct structures, *i.e.*, the protonated and deprotonated forms of FCCP. We emphasize that the conceptual difference between our approach and previous studies using extrinsic or intrinsic Raman tags in the silent region[6,7,14] is in the manner of utilizing the tag. Instead of using Raman tags to image the amount or concentration of a small molecule in live cells regardless of its structural state, in the present work, we used an intrinsic tag to simultaneously image different structural states of a given small molecule. Although FCCP was used as the model compound for this demonstration, the principle described here should be generally applicable to the structure-based imaging of various small molecules in live cells as a means of investigating their functional interactions.

This work was partly supported by a Grant-in-Aid for Young Scientists (B) (23710276 to H.Y.) from the Ministry of Education, Culture, Science, and Technology, Japan.

## Notes and references

1 (*a*) A. McFedries, A. Schwaid and A. Saghatelian, *Chem. Biol.*, 2013, **20**, 667; (*b*) S. Kumari and R. A. L. Van der Hoorn, *Curr. Opin. Plant Biol.*, 2011, **14**, 480; (*c*) S. Ziegler, V. Pries, C. Hedberg and H. Waldmann, *Angew. Chem., Int. Ed.*, 2013, **52**, 2744; (*d*) D. J. Newman and G. M. Cragg, *J. Nat. Prod.*, 2012, **75**, 311.

2 (*a*) N. Jamin, P. Dumas, J. Moncuit, W.-H. Fridman, J.-L. Teillaud, G. L. Carr and G. P. Williams, *Proc. Natl. Acad. Sci. U. S. A.*, 1998, **95**, 4837; (*b*) L. M. Miller and P. Dumas, *Biochim. Biophys. Acta*, 2006, **1758**, 846; (*c*) K. L. Munro, K. R. Bambery, E. A. Carter, L. Puskar, M. J. Tobin, B. R. Wood and C. T. Dillon, *Vib. Spectrosc.*, 2010, **53**, 39.

3 (*a*) R. E. Hester, *Anal. Chem.*, 1968, **40**, 320R; (*b*) D. L. Gerrard, *Anal. Chem.*, 1994, **66**, 547R; (*c*) J. M. Benevides, S. A. Overman and G. J. Thomas Jr, *J. Raman Spectrosc.*, 2005, **36**, 279; (*d*) R. Tuma, *J. Raman Spectrosc.*, 2005, **36**, 307; (*e*) B. L. N. Salmaso, G. J. Puppels, P. J. Caspers, R. Floris, R. Wever and J. Greve, *Biophys. J.*, 1994, **67**, 436; (*f*) B. R. Wood, B. Tait and D. McNaughton, *Biochim. Biophys. Acta*, 2001, **1539**, 58; (*g*) Y. Takai, T. Masuko and H. Takeuchi, *Biochim. Biophys. Acta*, 1997, **1335**, 199.

4 (*a*) J. Ye, S. A. Fox, M. Cudic, E. M. Rezler, J. L. Lauer, G. B. Fields and A. C. Terentis, *J. Am. Chem. Soc.*, 2010, **132**, 980; (*b*) A. Kaczor, K. Turnau and M. Baranska, *Analyst*, 2011, **136**, 1109; (*c*) G. Zhang, D. J. Moore, K. B. Sloan, C. R. Flach and R. Mendelsohn, *J. Invest. Dermatol.*, 2007, **127**, 1205; (*d*) G. Zhang, C. R. Flach and R. Mendelsohn, *J. Controlled Release*, 2007, **123**, 141; (*e*) Y. Harada, P. Dai, Y. Yamaoka, M. Ogawa, H. Tanaka, K. Nosaka, K. Akaji and T. Takamatsu, *Histochem. Cell Biol.*, 2009, **132**, 39.

5 (*a*) D. K. Veirs, J. W. Ager III, E. T. Loucks and G. M. Rosenblatt, *Appl. Opt.*, 1990, **29**, 4969; (*b*) M. Okuno and H. Hamaguchi, *Opt. Lett.*, 2010, **35**, 4096; (*c*) A. F. Palonpon, M. Sodeoka and K. Fujita, *Curr. Opin. Chem. Biol.*, 2013, **17**, 708; (*d*) L. Kong, P. Zhang, J. Yu, P. Setlow and Y. Li, *Appl. Phys. Lett.*, 2011, **98**, 213703.

6 (*a*) H. Yamakoshi, K. Dodo, M. Okada, J. Ando, A. Palonpon, K. Fujita, S. Kawata and M. Sodeoka, *J. Am. Chem. Soc.*, 2011, **133**, 6102; (*b*) A. F. Palonpon, J. Ando, H. Yamakoshi, K. Dodo, M. Sodeoka, S. Kawata and K. Fujita, *Nat. Protocols*, 2013, **8**, 677.

7 H. Yamakoshi, K. Dodo, A. Palonpon, J. Ando, K. Fujita, S. Kawata and M. Sodeoka, *J. Am. Chem. Soc.*, 2012, **134**, 20681.

8 (*a*) W. Kraemer, U. Schirmer, J. Peter and M. Witschle, *Modern Crop Protection Compounds*, Wiley-VCH, Weinhelm, 2nd edn, 2012, vol. 2, pp. 154–645; (*b*) V. P. Skulachev, *Biochim. Biophys. Acta*, 1998, **1363**, 100.

9 P. G. Heytler and W. W. Prichard, *Biochem. Biophys. Res. Commun.*, 1962, **7**, 272.

10 Y. N. Antonenko, A. V. Avetisyan, D. A. Cherepanov, D. A. Knorre, G. A. Korshunova, O. V. Markova, S. M. Ojova, I. V. Perevoshchikova, A. V. Pustovidko, T. I. Rokitskaya, I. L. Severina, R. A. Simonyan, E. A. Smirnova, A. A. Sobko, N. V. Sumbatyan, F. F. Severin and V. P. Skulachev, *J. Biol. Chem.*, 2011, **286**, 17831.

11 J. C. Merlin, E. W. Thomas and G. Petit, *Can. J. Chem.*, 1985, **63**, 1840.

12 (*a*) K. Hamada, K. Fujita, N. I. Smith, M. Kobayashi, Y. Inoue and S. Kawata, *J. Biomed. Opt.*, 2008, **13**, 044027; (*b*) T. G. Spiro and T. C. Strekas, *Proc. Natl. Acad. Sci. U. S. A.*, 1972, **69**, 2622.

13 (*a*) F. Legros, A. Lombes, P. Frachon and M. Rojo, *Mol. Biol. Cell*, 2002, **13**, 4343; (*b*) C. Sauvanet, S. D. Caubet, J.-P. di Rago and M. Rojo, *Semin. Cell Dev. Biol.*, 2010, **21**, 558.

14 K. Meister, J. Niesel, U. Schatzschneider, N. Metzer-Nolte, D. A. Schmidt and M. Havenith, *Angew. Chem., Int. Ed.*, 2010, **49**, 3310.